



# Clinical value of $^{99}\text{Tc}^{\text{m}}$ -MIBI gated myocardial perfusion imaging in evaluating sarcoglycanopathy

Peng Fu<sup>1</sup>, Ling-Ge Wei<sup>1</sup>, Jing Hu<sup>2</sup>, Jian-Qing Gao<sup>1,2</sup>, Jian-Min Jing<sup>1</sup>, Xiao-Mei Liu<sup>1</sup>, Jian-Min Huang<sup>1</sup>

<sup>1</sup>Department of Nuclear Medicine, Third Hospital of Hebei Medical University, Shijiazhuang, China

<sup>2</sup>Department of Neuromuscular Disorders, Third Hospital of Hebei Medical University, Shijiazhuang, China

## ABSTRACT

**Aim.** The purpose of this study was to analyse the diagnostic value of gated myocardial perfusion imaging (G-MPI) in the evaluation of myocardial injury in sarcoglycanopathy.

**Materials and methods.** Twenty-eight patients diagnosed with sarcoglycanopathy were evaluated using  $^{99}\text{Tc}^{\text{m}}$ -methoxyisobutylisonitrile ( $^{99}\text{Tc}^{\text{m}}$ -MIBI) G-MPI. The data was processed into tomographic images, and the left ventricular function was analysed using quantitative gated SPECT (QGS) to assess the degree of impairment in myocardial and cardiac function.

**Results.** The images of 23 of the patients (82.1%) were positive. Two hundred and twenty-nine sub-segments with abnormal lesions were detected out of 391 cardiac sub-segments of these 23 positive cases. According to the segmental abnormalities, the cases were divided into two cases (8.7%) with single abnormal wall segment, six cases (26.1%) with two abnormal wall segments, and 15 cases (65.2%) with three or more abnormal wall segments or scattered lesions.

**Conclusions.**  $^{99}\text{Tc}^{\text{m}}$ -MIBI G-MPI can objectively show impaired myocardium in patients with sarcoglycanopathy. Therefore, this method is helpful for early diagnosis and follow-up of myocardial damage.

**Key words:** Sarcoglycanopathy, tomography, emission computer, single photon, MIBI

(*Neurol Neurochir Pol* 2019; 53 (4): 265–270)

## Introduction

Sarcoglycanopathy is the general term used to describe limb-girdle muscular dystrophy (LGMD) (2D, 2E, 2C, and 2F), which is caused due to defects in the expression of the four subunits of myosin protein:  $\alpha$ -,  $\beta$ -,  $\gamma$ -, and  $\delta$  [1, 2]. The coding genes for  $\alpha$ -,  $\beta$ -,  $\gamma$ -, and  $\delta$  subunits of myosin protein are SGCA(17q21), SGCB(4q12), SGCG(13q12), and SGCD(5q33), respectively. LGMD refers to a group of hereditary skeletal muscle diseases with the main clinical manifestations being amyosthenia and progressive aggravated myotrophy in the proximal extremity and lumbar muscles [3–5]. Both the myocardium and the skeletal muscles belong to the striated muscle, and they are differentiated from the mesenchymal cells. The mesenchymal cells first differentiate into the myoblasts, and then differentiate into the myocytes and the skeletal muscle cells differently [6]. Due to these common histologic and embryologic features, genetic or metabolic diseases that

affect the skeletal muscle fibres may cause myocardial damage by affecting the structure, function, or metabolism of the cardiac muscle cells.

At present, studies on cardiac injury in sarcoglycanopathy are mostly focused on electrocardiograms or echocardiography. For example, ultrasound is used to measure the changes in thickness of the atrophied muscles [7], or to diagnose and evaluate the efficacy of myocardial dystrophy [8]. The advantage of magnetic resonance imaging (MRI) is that it can access the energy metabolism and function of the heart, which is important information about the early stages of myocardial damage in muscular dystrophy [9]. Radionuclide myocardial imaging can simultaneously display myocardial metabolism and blood flow distribution. It is also used in determining the existence of myocardial ischaemia as well as the ischaemic site and scope, detecting myocardial survival, and understanding the wall movement and the left ventricular function [10]. However, few studies have been conducted into applying

**Address for correspondence:** Ling-Ge Wei, Department of Nuclear Medicine, The Third Hospital of Hebei Medical University, Shijiazhuang, China, e-mail: linggewei@126.com

radionuclide myocardial imaging in evaluating myocardial damage in sarcoglycanopathy.

In this study,  $^{99m}\text{Tc}$ -methoxyisobutylisonitrile ( $^{99m}\text{Tc}$ -MIBI) gated myocardial perfusion imaging (G-MPI) was performed on 13 patients with myopathy (the CON group) and 28 patients with sarcoglycanopathy (the SAR group) diagnosed through clinical, routine pathological staining, and immunohistochemical staining of muscle biopsy in our hospital. The aim was to analyse the value of gated myocardial tomography in evaluating myocardial damage and heart function in patients with sarcoglycanopathy.

## Materials and methods

### Clinical data

Twenty-eight patients with sarcoglycanopathy diagnosed through clinical, routine pathological staining, and immunohistochemical staining of muscle biopsy in the Department of Neuromuscular Diseases of our hospital from September 2008 to July 2017 were enrolled in the study, including 17 males and 11 females, aged 8–30 years, with an average age of  $15.3 \pm 4.1$  years. The CON group was composed of 13 patients, aged  $16.5 \pm 3.9$  years. The diagnosis was based on the clinical manifestations of amyosthenia and progressive aggravated myotrophy in the proximal extremity muscles. All 28 patients in the SAR group had different levels of elevated blood CK ( $366$  to  $8,270$  IU/L) and exhibited myogenic injury in the electromyograms. All patients were further confirmed through skeletal muscle biopsy and immunohistochemical staining. The 13 patients in the CON group were collected from the Department of Neuromuscular Diseases and clinically newly diagnosed with myopathy while excluding patients with sarcoglycanopathy, Duchenne, or Becker muscular dystrophy through skeletal muscle biopsy, immunohistochemical staining, and pathological analysis. Heart colour Doppler ultrasound and electrocardiogram examination revealed no abnormality in the heart. This study was conducted in accordance with the Declaration of Helsinki. This study was conducted with approval from the Ethics Committee of Hebei Medical University. Written informed consent was obtained from all participants.

### Imaging data collection

Each studied subject was intravenously injected with  $111\text{-}740\text{MBq}$   $^{99m}\text{Tc}$ -MIBI ( $^{99m}\text{Tc}$ , HTA Co., Ltd; MIBI, Beijing Shihong Pharmaceutical Centre) (radiochemical purity  $> 95\%$ ) in fasting and resting conditions. The dosing method was as follows: dosage = body weight (kg) /  $70 \times$  adult dose [11]. Thirty minutes later,  $150\text{--}200$  ml of milk was administered, and gated myocardial perfusion imaging was performed 1.5h later. The imaging apparatus used here was the Infinia VC Hawkeye dual-head single-photon emission-computed tomography (SPECT, GE, USA), together with a low-energy, high-resolution collimator. The acquisition conditions and

methods were referred to the reference [11]. The electrocardiographic R-wave was used to trigger the gated synchronous acquisition (8 frames per cycle with the matrix as  $64 \times 64$ ). Image analysis and processing were performed using the Xeleris functional imaging processing station (GE, USA); the image reconstruction used the filtered back projection method with Butterworth as the filter function and the system-recommended cutoff frequency and steepness factor. Images of the short, vertical long and horizontal long axis were shown after reconstruction. Quantitative gated SPECT (QGS) software was used to analyse the left ventricular ejection fraction (LVEF), end-diastolic volume (EDV), and end-systolic volume (ESV).

### Image processing and result analysis

The left ventricle is divided into seven segments (the cardiac apex, anterior, anterolateral, inferolateral, inferior, inferior septum, and anterior septum wall) and 17 subsegments, including the cardiac apical, the proximal cardiac apical (anterior, septum, inferior, and lateral wall), the proximal basement (anterior, anterior interarticular, inferior interarticular, inferior, inferolateral, and anterolateral wall), and the basement (anterior, anterior interarticular, inferior interarticular, inferior, inferolateral, and anterolateral wall) subsegments. In addition, the radioactivity of each segment was scored using one 5-point scoring method (i.e. from 0 to 4 points) as follows: 0 point = normal radioactivity distribution, 1 point = mild decreased uptake, 2 points = moderate decreased uptake, 3 points = severe decreased uptake, 4 points = no radioactive uptake. According to the number of lesion-involved segments, mild lesions were limited to one segment, moderate lesions involved two segments, and severe lesions involved three segments. All the images were determined by two or more experienced nuclear medicine practitioners.

## Results

### Pathological analysis of skeletal muscle biopsy

Histochemical staining: All the 28 patients showed pathological changes of muscular dystrophy, together with different sizes of muscular fibre, different degrees of muscular fibre necrosis and regeneration, scattered opaque muscle fibres, hyperplasia, degeneration necrosis of connective tissue, myofibre regeneration, and obvious connective tissue hyperplasia (Fig. 1).

The immunohistochemical staining of the skeletal muscle biopsies of the SAR group of 28 patients showed attenuation/defects in the expression of  $\alpha$ -, b-, g-, and d-sarcoglycan proteins on the myofibril membranes (by immunohistochemical staining of anti- $\alpha$ -, b-, g-, and d-sarcoglycan monoclonal antibodies), as shown in Figure 2.

### G-MPI

The results of  $^{99m}\text{Tc}$ -MIBI G-MPI in the CON group showed that the thickness of the myocardium of the left ventricle was uniform, and the radioactivity of each segment was evenly

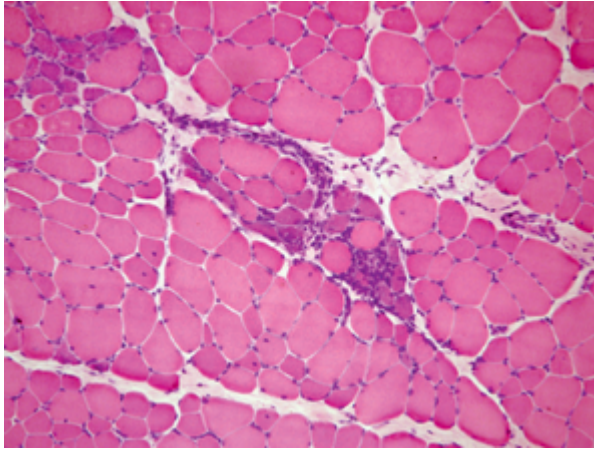


**Figure 1.** Pathological changes of skeletal muscle biopsy: varying muscle fibre sizes, varying degrees of muscle fibre necrosis/regeneration, scattered opaque muscle fibres, proliferation, degeneration, and necrosis of connective tissue, or myofibre regeneration (HE staining  $\times 100$ )

distributed and had no sparse or defective area. The overall function of the left ventricle was normal.

Among the 28 patients in the SAR group, the results of  $^{99m}\text{Tc}$ -MIBI G-MPI were positive in 23 patients, and the positive rate was 82.1% (23/28). Two hundred and twenty-nine subsegments with abnormal lesions were detected from the 391 subsegments of these 23 patients. According to the distribution of intra-myocardial radioactivity, the radionuclide distribution slightly decreased in 88 subsegments (1 point, 38.4%), moderately decreased in 73 subsegments (2 points, 31.9%), severely decreased in 50 subsegments (3 points,

21.8%), and no radioactivity distribution in 18 subsegments (4 points, 7.9%). According to the number of involved sites, among the 229 diseased subsegments, 41 subsegments were located at the apex, 39 subsegments were located at the anterior wall, 32 subsegments were located at the anterolateral wall, 28 subsegments were located at the inferolateral wall, 31 subsegments were located at the inferior wall, 33 subsegments were located at the inferior interarticular wall, and 25 subsegments were located at the anterior interarticular wall. Six cases exhibited abnormality in two wall segments (mild, 8.7%), two cases exhibited abnormality in three or more wall segments (medium, 26.1%), and 15 cases showed scattered lesion distribution (severe, 65.2%) (the typical cases are shown in Figure 3).

### Left ventricular functional parameters

In the CON group, LVEF was  $56.3 \pm 3.2\%$ , EDV was  $96.7 \pm 7.2$  ml, and ESV was  $40.4 \pm 6.4$  ml. Among the 23 patients that exhibited positive results with myocardial perfusion imaging, seven patients showed elevated left ventricular EDV and ESV (EDV  $132.3 \pm 11.7$  ml, ESV  $74.6 \pm 9.6$  ml), and four patients showed decreased LVEF  $42.8 \pm 2.3\%$  with poor coordination of diffuse movement of the left ventricular wall (Fig. 4 for typical cases). The five patients with negative results of myocardial perfusion imaging showed normal LVEF, EDV, and ESV.

### Discussion

Sarcoglycanopathy is a hereditary skeletal muscle disease with progressive aggravated amyosthenia and myatrophy as the main clinical manifestations, which gradually aggravates with the prolongation of the disease course. Amyosthenia and

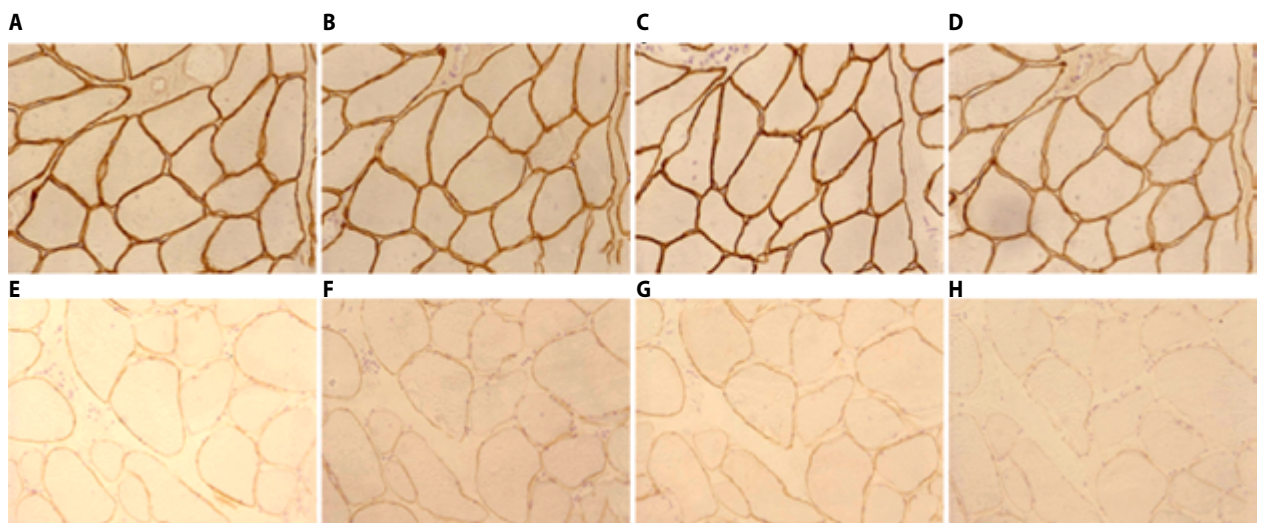


**Figure 2.** Pathological analysis of immunohistochemical staining. A–D: Patients in the CON group (patients with LGMD2B): immunohistochemical staining of anti- $\alpha$ -, b-, g-, and d- monoclonal antibodies shows the subunit proteins of sarcoglycan are expressed normally ( $\times 500$ ); E–H: patients in the SAR group (patients with LGMD2F): immunohistochemical staining of anti- $\alpha$ -, b-, g-, and d- monoclonal antibodies shows the subunit proteins of d-sarcoglycan is obviously reduced, and other subunit proteins are downregulated ( $\times 500$ )



myotrophy usually become apparent in the first or second decades. Progressive aggravated amyosthenia makes actions become more difficult, together with gradually developed and aggravated myocardial damage as the disease progresses. This will seriously affect the quality of life of the patient and place heavy economic and social burdens upon individuals, families, and society. Therefore, early detection, necessary interventions, and dynamic observation of the prognosis of myocardial lesions are crucial [12–14].

At present, there are a few studies on cardiac diseases caused by sarcoglycanopathy [15], which are mostly detected using electrocardiograms and colour ultrasound. Studies have reported that the myocardium can be affected by sarcoglycanopathy, and sometimes appears as dilated cardiomyopathy in echocardiography [15]. Studies using  $^{99}\text{Tc}^{\text{m}}$ -MIBI G-MPI in evaluating myocardial damage in patients with sarcoglycanopathy are rare. In this study,  $^{99}\text{Tc}^{\text{m}}$ -MIBI G-MPI was performed on patients clinically diagnosed with sarcoglycanopathy, aiming to explore preliminarily the diagnostic value of this technique on myocardial lesions in patients with sarcoglycanopathy.

Of the 28 patients enrolled in this study, 23 patients exhibited positive results. The histological features of the myocardium are similar to those of skeletal muscles, as both are striated muscles and contain sarcolemmal proteins. In the case of sarcoglycanopathy,  $\alpha$ -,  $\beta$ -,  $\gamma$ -, and  $\delta$ -sarcoglycan form a sarcoglycan complex in the dystrophin glycoprotein complex, which is important in stabilising the cytoskeleton of the muscle and has the function of maintaining the cell membrane stability. The loss of any of these functions can result in the attenuation and disappearance of the complex protein on the cell membrane. The defect of one component of the complex causes the obstruction of the synthesis and assembly process of other proteins on the sarcolemmal membrane, which may impair the integrity and stability of the sarcolemma structure, followed by the degeneration and necrosis of muscular cells [16]. The myocardial uptake of  $^{99}\text{Tc}^{\text{m}}$ -MIBI is closely related to the integrity of the myocardial cell membrane [17], which in turn affects the uptake of  $^{99}\text{Tc}^{\text{m}}$ -MIBI by the cardiac myocytes, resulting in abnormal changes such as sparseness. The defect in the complex protein may be an important pathogenic factor for sarcoglycanopathy combined with cardiomyopathy.

The degeneration and necrosis of cardiomyocytes in patients with sarcoglycanopathy occur and disperse in multiple sites. The characteristic of its myocardial perfusion imaging appears to be scattered multiple focal lesions (mostly multilaminar myocardial involvement), patchy myocardium, and non-segmental (having nothing to do with the shape of the coronary artery, and different from coronary artery stenosis-resulted myocardial ischaemia in the coronary artery-dominating area).  $^{99}\text{Tc}^{\text{m}}$ -MIBI imaging can objectively reflect whether the myocardial cell function is normal [17]. Therefore, this study can objectively reflect myocardial ischaemia caused by paediatric coronary artery disease. The changes in cardiac

function found in this study focused on patients with multi-wall lesions; the severity of myocardial damage as well as the state of cardiac function may be related to the extent and the course of such pathological changes as in myofibre necrosis and connective tissue hyperplasia.

Among the 28 patients, five exhibited negative results with  $^{99}\text{Tc}^{\text{m}}$ -MIBI G-MPI. The explanation may be that recent studies have found that sarcoglycan has other subunits, namely  $\epsilon$  and  $\zeta$ -sarcoglycan. These two subunits are mainly found in the smooth muscle but distribute only in small amounts in the skeletal muscle [18]. The defective subunit protein of sarcoglycanopathy determines the degree of involvement of myocardial lesions. If the defective subunit protein is predominantly distributed in the skeletal muscle but in a small amount in the myocardium, an obvious defect of this subunit protein may be found in the skeletal muscle by immunohistochemical staining while myocardial damage may be milder. This may be determined by the subunit protein. With the differences in the subunit proteins, the clinical phenotypes may be different. Politano et al. [19] performed electrocardiography, echocardiography, and pulmonary function assessments on 20 patients with sarcoglycanopathy and found that 31.3% of the patients had normal cardiac function, 43.7% had subclinical myocardium disease, 6.3% of patients had arrhythmia myocardium disease, and 18.7% showed dilated cardiomyopathy. Hypoxic myocardial damage occurring at  $\beta$ ,  $\gamma$ , and  $\delta$ , and  $\gamma$  and  $\delta$  normally shows changes in the dilated cardiomyopathy. Fayssoil et al. [20] compared the cardiac function data of eight patients with  $\alpha$ -type sarcoglycanopathy and that of 11 patients with  $\gamma$ -type sarcoglycanopathy using echocardiography, and found that the cardiac function in patients with  $\gamma$ -type sarcoglycanopathy is more vulnerable compared to that of patients with  $\alpha$ -type sarcoglycanopathy (LVEF:  $45.6 \pm 1.8\%$  vs.  $59.6 \pm 5.9\%$ ,  $P = 0.018$ ). In addition, it may be related to the course of the disease to certain extent.

In this study, the positive rate of  $^{99}\text{Tc}^{\text{m}}$ -MIBI G-MPI was 82.1%. This inspection method is safe, non-invasive, and repeatable. The limitations of this study are that the results were affected by the types of disease, and the number of cases was limited. Our future studies will gradually increase the case number. Some hereditary and metabolic skeletal muscle diseases involve the myocardium and are relatively invisible in the early stages. Late-stage revealing is one of the most important causes of death in such patients. When the pathological changes of the skeletal muscle are involved, myocardial involvement should not be spared.  $^{99}\text{Tc}^{\text{m}}$ -MIBI gated myocardial perfusion tomography can dynamically show myocardial lesions, thus providing as early diagnosis and intervention as possible so as to improve the survival of such patients. The  $^{99}\text{Tc}^{\text{m}}$ -MIBI myocardial rest imaging can visually show the location, extent, and degree of the diseased myocardium, thus providing great help for the judgment of clinical condition. Therefore, as a routine, simple, non-invasive, and high-diagnostic method, it has a high value, which can be used not only for early diagnosis of myocardial injury, but also for long-term follow-up studies.

**Acknowledgements:** *This work was supported by the Research Project of Excellent Talents in Clinical Medicine funded by Hebei Provincial Government.*

**Conflicts of interest:** *The authors declare no conflict of interest.*

## References

- Liewluck T, Milone M. Untangling the complexity of limb-girdle muscular dystrophies. *Muscle Nerve*. 2018; 58(2): 167–177, doi: [10.1002/mus.26077](https://doi.org/10.1002/mus.26077), indexed in Pubmed: [29350766](https://pubmed.ncbi.nlm.nih.gov/29350766/).
- Petnikota H, Madhuri V, Gangadharan S, et al. Retrospective cohort study comparing the efficacy of prednisolone and deflazacort in children with muscular dystrophy: A 6 years' experience in a South Indian teaching hospital. *Indian J Orthop*. 2016; 50(5): 551–557, doi: [10.4103/0019-5413.189609](https://doi.org/10.4103/0019-5413.189609), indexed in Pubmed: [27746500](https://pubmed.ncbi.nlm.nih.gov/27746500/).
- Cox ML, Evans JM, Davis AG, et al. Exome sequencing reveals independent SGCD deletions causing limb girdle muscular dystrophy in Boston terriers. *Skelet Muscle*. 2017; 7(1): 15, doi: [10.1186/s13395-017-0131-0](https://doi.org/10.1186/s13395-017-0131-0), indexed in Pubmed: [28697784](https://pubmed.ncbi.nlm.nih.gov/28697784/).
- Ghafouri-Fard S, Hashemi-Gorji F, Fardaei M, et al. Limb girdle muscular dystrophy type 2E due to a novel large deletion in SGCB gene. *Iran J Child Neurol*. 2017; 11(3): 57–60, indexed in Pubmed: [28883879](https://pubmed.ncbi.nlm.nih.gov/28883879/).
- Mojbafan M, Nilipour Y, Tonekaboni SH, et al. A rare form of limb girdle muscular dystrophy (type 2E) seen in an Iranian family detected by autozygosity mapping. *J Neurogenet*. 2016; 30(1): 1–4, doi: [10.3109/01677063.2016.1141208](https://doi.org/10.3109/01677063.2016.1141208), indexed in Pubmed: [27276190](https://pubmed.ncbi.nlm.nih.gov/27276190/).
- Lerman DA, Alotti N, Ume KL, et al. Cardiac repair and regeneration: the value of cell therapies. *Eur Cardiol*. 2016; 11(1): 43–48, doi: [10.15420/ecr.2016.8:1](https://doi.org/10.15420/ecr.2016.8:1), indexed in Pubmed: [27499812](https://pubmed.ncbi.nlm.nih.gov/27499812/).
- Ferreira B, Da Silva GP, Gonçalves CR, et al. Stomatognathic function in Duchenne muscular dystrophy: a case-control study. *Dev Med Child Neurol*. 2016; 58(5): 516–521, doi: [10.1111/dmcn.13094](https://doi.org/10.1111/dmcn.13094), indexed in Pubmed: [26991937](https://pubmed.ncbi.nlm.nih.gov/26991937/).
- Spurney CF, McCaffrey FM, Cnaan A, et al. Feasibility and reproducibility of echocardiographic measures in children with muscular dystrophies. *J Am Soc Echocardiogr*. 2015; 28(8): 999–1008, doi: [10.1016/j.echo.2015.03.003](https://doi.org/10.1016/j.echo.2015.03.003), indexed in Pubmed: [25906753](https://pubmed.ncbi.nlm.nih.gov/25906753/).
- Franco A, Javidi S, Ruehm SG. Delayed myocardial enhancement in cardiac magnetic resonance imaging. *J Radiol Case Rep*. 2015; 9(6): 6–18, doi: [10.3941/jrcr.v9i6.2328](https://doi.org/10.3941/jrcr.v9i6.2328), indexed in Pubmed: [26622933](https://pubmed.ncbi.nlm.nih.gov/26622933/).
- Fu P, Hu L, Sinzinger J, et al. Assessment of cardiac abnormalities in Duchenne's muscular dystrophy by (99m)Tc-MIBI gated myocardial perfusion imaging. *Hell J Nucl Med*. 2012; 15(2): 114–119, indexed in Pubmed: [22833857](https://pubmed.ncbi.nlm.nih.gov/22833857/).
- Zhang Li, Liu Z, Hu KY, et al. Early myocardial damage assessment in dystrophinopathies using (99)Tc(m)-MIBI gated myocardial perfusion imaging. *Ther Clin Risk Manag*. 2015; 11: 1819–1827, doi: [10.2147/TCRM.S89962](https://doi.org/10.2147/TCRM.S89962), indexed in Pubmed: [26677332](https://pubmed.ncbi.nlm.nih.gov/26677332/).
- Khadiolkar SV, Faldu HD, Patil SB, et al. Limb-girdle muscular dystrophies in india: a review. *Ann Indian Acad Neurol*. 2017; 20(2): 87–95, doi: [10.4103/aian.AIAN\\_81\\_17](https://doi.org/10.4103/aian.AIAN_81_17), indexed in Pubmed: [28615891](https://pubmed.ncbi.nlm.nih.gov/28615891/).
- Liang WC, Chou PC, Hung CC, et al. Probable high prevalence of limb-girdle muscular dystrophy type 2D in Taiwan. *J Neurol Sci*. 2016; 362: 304–308, doi: [10.1016/j.jns.2016.02.002](https://doi.org/10.1016/j.jns.2016.02.002), indexed in Pubmed: [26944168](https://pubmed.ncbi.nlm.nih.gov/26944168/).
- Dalichaouche I, Sifi Y, Roudaut C, et al.  $\gamma$ -sarcoglycan and dystrophin mutation spectrum in an Algerian cohort. *Muscle Nerve*. 2017; 56(1): 129–135, doi: [10.1002/mus.25443](https://doi.org/10.1002/mus.25443), indexed in Pubmed: [27759885](https://pubmed.ncbi.nlm.nih.gov/27759885/).
- Schade van Westrum SM, Dekker LRC, de Voogt WG, et al. Cardiac involvement in Dutch patients with sarcoglycanopathy: a cross-sectional cohort and follow-up study. *Muscle Nerve*. 2014; 50(6): 909–913, doi: [10.1002/mus.24233](https://doi.org/10.1002/mus.24233), indexed in Pubmed: [24619517](https://pubmed.ncbi.nlm.nih.gov/24619517/).
- Moorwood C, Philippou A, Spinazzola J, et al. Absence of  $\gamma$ -sarcoglycan alters the response of p70S6 kinase to mechanical perturbation in murine skeletal muscle. *Skelet Muscle*. 2014; 4: 13, doi: [10.1186/2044-5040-4-13](https://doi.org/10.1186/2044-5040-4-13), indexed in Pubmed: [25024843](https://pubmed.ncbi.nlm.nih.gov/25024843/).
- Masuda A, Yoshinaga K, Naya M, et al. Accelerated (99m)Tc-sestamibi clearance associated with mitochondrial dysfunction and regional left ventricular dysfunction in reperfused myocardium in patients with acute coronary syndrome. *EJNMMI Res*. 2016; 6(1): 41, doi: [10.1186/s13550-016-0196-5](https://doi.org/10.1186/s13550-016-0196-5), indexed in Pubmed: [27169534](https://pubmed.ncbi.nlm.nih.gov/27169534/).
- Reddy HM, Hamed SA, Lek M, et al. Homozygous nonsense mutation in SGCA is a common cause of limb-girdle muscular dystrophy in Assiut, Egypt. *Muscle Nerve*. 2016; 54(4): 690–695, doi: [10.1002/mus.25094](https://doi.org/10.1002/mus.25094), indexed in Pubmed: [26934379](https://pubmed.ncbi.nlm.nih.gov/26934379/).
- Politano L, Nigro V, Passamano L, et al. Evaluation of cardiac and respiratory involvement in sarcoglycanopathies. *Neuromuscul Disord*. 2001; 11(2): 178–185, indexed in Pubmed: [11257475](https://pubmed.ncbi.nlm.nih.gov/11257475/).
- Faysoil A, Nardi O, Annane D, et al. Left ventricular function in alpha-sarcoglycanopathy and gamma-sarcoglycanopathy. *Acta Neurol Belg*. 2014; 114(4): 257–259, doi: [10.1007/s13760-013-0276-5](https://doi.org/10.1007/s13760-013-0276-5), indexed in Pubmed: [24464767](https://pubmed.ncbi.nlm.nih.gov/24464767/).